

MULTIFRACTAL CHARACTERISTICS OF VERTICAL AND HORIZONTAL APPARENT ELECTRICAL CONDUCTIVITY MEASURED ALONG REPLICATED TRANSECTS

M. Valcárcel Armesto¹, J. R. Raposo González¹, J. Dafonte Dafonte¹, R. da Silva Dias², E. Vidal Vázquez² and A. Paz González²

¹ Departamento de Ingeniería Agroforestal, Escuela Politécnica Superior, Universidad de Santiago de Compostela, Campus Universitario, 27002, Lugo, e-mail: montse.valcarcel@usc.es, web: <http://www.proepla.es>

² Facultad de Ciencias, Universidad de A Coruña, Campus A Zapateira, 15008, A Coruña. e-mail: tucho@udc.es

RESUMEN. La conductividad eléctrica aparente (ECa) se utiliza para conocer la variabilidad intrínseca al, que a su vez, permite mejorar la evaluación de la variabilidad espacial y temporal de algunas propiedades físicas y químicas del suelo. El objetivo de este trabajo consistió en caracterizar la heterogeneidad espacial de sucesivas medidas de CEa llevadas a cabo sobre un pequeño transecto, de unos 52 m. Las medidas se llevaron a cabo en una parcela situada en la finca experimental del CIAM en Mabegondo, A Coruña, España. A lo largo del perfil se registró la conductividad eléctrica aparente en continuo, tanto con el dipolo en orientación vertical (ECa-V) como en posición horizontal (ECa-H). La medición de estas magnitudes se repitió durante cinco veces sucesivas. Se puso de manifiesto la naturaleza multifractal de ECa, de modo que las regiones con baja y alta densidad de esta variable presentan distintos modos de escalamiento. Se comprobó que diversos parámetros obtenidos del espectro de singularidad y del espectro de dimensiones generalizadas de ECa-V y ECa-H no presentaban diferencias estadísticas significativas ($P < 0.05$) en ninguna de las sucesivas mediciones repetidas. Por el contrario, estos parámetros multifractales presentaron diferencias significativas cuando se compararon entre sí mediciones sucesivas efectuadas a lo largo del transecto estudiado.

ABSTRACT. Apparent electrical conductivity (ECa) is widely used either to assess intrinsically soil variability to better assess the spatial and temporal variability in several soil chemical and physical properties. The aim of this study was to characterize the scaling properties of replicated soil ECa measurements performed along a short transect of about 52 m. Field measurements were carried out at the experimental farm of CIAM located in Mabegondo, A Coruña, Spain. Apparent electrical conductivity was continuously recorded along the profile both in the vertical (ECa-V) and horizontal (ECa-H) dipole orientations. Five successive repetitions of the measurement were carried out. The scaling properties of all the data sets studied implied a multifractal nature, where the low and high density regions of ECa scale differently. Statistical analysis showed that several parameters gathered from singularity spectrum and the generalized dimension spectrum were not significantly different ($P < 0.05$) between ECa-V and ECa-H for any of the studied repetitions. In contrast, multifractal parameters were significantly different when successive repetitions recorded along the transect studied were compared.

1.- Introduction

The apparent electrical conductivity (ECa) of the soil and/or the vadose zone mainly depends on soil moisture content and on electrolyte concentration of the soil solution (Lesch et al., 1995). In addition, EC_a can be also influenced by several physical and chemical factors of the soil profile, including soil porosity, clay content and its mineralogy and organic matter content (e.g. Corwin and Lesch, 2005; Shimulik, 2005; Martínez et al., 2009). The use of soil ECa as a substitute for detection and mapping of spatial variation in soil chemical and physical properties has been demonstrated to be an adequate method. Several reviews concerning the use of ECa to estimate soil properties are available (e.g. Corwin and Lesch 2005; Shimulik, 2005; Allred et al., 2008).

On the other hand, scaling analysis, such as fractal and multifractal analysis, has been frequently used to adequately characterize the spatial variability of soil properties and to describe the combination of irregularity and structure of such properties for a large range of scales. Both, fractal and multifractal scaling assume a hierarchical distribution of mass in space, so that the whole results from the union of similar subsets (e.g. Caniego et al., 2005; Tarquis et al., 2008). While in monofractal scaling one single exponent is sufficient to capture the scaling behavior of the studied data set, multifractal scaling involves entire functions, which represents a hierarchy of exponents related to different levels of intensity or irregularities of the data series (Everstz and Mandelbrot, 1992; Falconer, 1997). Thus, multifractals are intrinsically more complex and inhomogeneous than monofractals.

Commercial devices are available to economically and rapidly measure and map bulk soil EC across agricultural field. The EM38 (Geonics, Limited, Mississauga, Ontario, Canada) induces a current into the soil with one coil and determines conductivity by measuring the resulting secondary current with another coil. Using this device ECa measurements can be taken either at selected points or continuously recorded along transects.

Pearson product moment correlation is the most common method employed to assess linear relationships between ECa data sets taken at fixed locations and different times

and also to compare results provided by data sets obtained at vertical and horizontal dipole positions. Continuous record of ECa provides very detailed information with distances between readings at the decimeter scale. However the automatic data collection process produces data sets with more or less noise that is the result of low-level data errors. Moreover, in current surveys it is hardly possible to automatically record ECa values at exactly the same points along a transect when measurements are performed at different times. The multifractal approach could be useful to characterize the inner structure of ECa data sets recorded automatically and to compare reading taken by EM38 at different times or with the two coil configurations. Therefore, the objective of this research was to characterize successive ECa readings continuously recorded, both in vertical and horizontal dipole positions, along a transect using multifractal analysis.

2.- Material and methods

2.1.- Experimental site and soil CEa data set

The CEa data sets were measured at an experimental field of the “Centro de Investigaciones Agrarias de Mabegondo” (CIAM), A Coruña province, Spain, (Latitude 43° 14' 47" N, Longitude 8° 16' 23" W). The site was on a gentle slope and the soil was a loamy textured Inceptisol.

The data sets of ECa were continuously recorded and collected in conjunction with mobile RTK DGPS-based system that continuously recorded the values of electromagnetic induction. The measurement campaign was undertaken in may 2010. The EM38 was placed both in the vertical coil configuration (ECa-H), where its effective signal detection ($\pm 70\%$ of the response) is from 1.5 m, and in the vertical coil configuration (ECa-V) with an effective signal detection depth of 0.75 m (Geonics Limited 1999). Five profiles in each dipole orientation (ECa-V ECa-H) were successively recorded. The total duration of the automatic ECa measurements in field conditions was at about three hours. Raw data were corrected to take into account effects of temperature oscillations during the measurement period.

2.2.- Multifractal analysis

Multifractal analysis was implemented following the moment method, which is next summarized. First, a mesh or segment with size δ are required to be superimposed over the whole support. In other words, the length of the transect was divided into smaller and smaller segments based on dyadic downscaling. This was implemented by successive partitions of the support in k stages ($k=1, 2, 3\dots$) that generate at each scale, δ , a number of segments, $N(\delta) = 2^k$ of characteristic size length, $\delta = L \times 2^{-k}$, covering the whole extent of the support, L , in this case as a transect (e.g. Evertsz and Mandelbrot, 1992; Vidal et al., 2013).

Then, the experimental data for each ECa data set were converted into the distribution of mass along the geometric support. Therefore, the probability mass function, $p_i(\delta)$, for each segment was estimated as a proportion according to:

$$p_i(\delta) = \frac{N_i(\delta)}{N_t} \quad (1)$$

Where $N_i(\delta)$ is the value of the measure in a given segment, i^{th} , and N_t is the sum of the measure in the whole transect.

Multifractal analysis involves several scaling functions: mass exponent, τ_q , singularity spectrum, $f(\alpha)$, local scaling index, α_q , and generalized or Rényi dimension, D_q . In practice, using the box counting method, the so-called partition function scales with the segment size as follows:

$$\chi(q, \delta) = \sum_{i=1}^{n(\delta)} p_i^q(\delta) \quad (2)$$

Where $n(\delta)$ is the number of segments with size δ , and statistical moments q are defined for $-\infty < q < \infty$.

A log-log plot of the quantity $\chi(q, \delta)$ versus δ for different values of q yields: $\chi(q, \delta) \propto \delta^{-\tau(q)}$, where τ_q is the mass scaling function of order q . Note that the method of moments is justified if the plots of $\chi(q, \delta)$ versus δ are straight lines (Halsey et al., 1986).

The mass exponent function τ_q was estimated from the partition function as:

$$\tau(q) = \lim_{\delta \rightarrow 0} \frac{\log \chi(q, \delta)}{\log(1/\delta)} \quad (3)$$

The function τ_q controls how the moment of measure μ_i scales with q . In general, multifractal measures yield a nonlinear function of τ_q , whereas a monofractal corresponds to linear τ_q .

For each box or segment, the probability distribution is: $p_i(\delta) = \delta^{\alpha_i}$, where α_i is the singularity or Hölder exponent characterizing density in the i^{th} box (Halsey et al., 1986). The Hölder exponent, given by $\alpha_i = \log \mu_i(\delta) / \log \delta$, may be interpreted as a crowding index for the degree of concentration of the measure, μ . It is, in fact, the logarithmic density of the i -th box of the partition of characteristic size δ .

For multifractal distributed measures, the number $N_\delta(\alpha)$ of cells of size δ , having a singularity or Hölder exponent equal to α , increases for decreasing δ and obeys a power law: $N(\alpha) \propto \delta^{-f(\alpha)}$, where the exponent $f(\alpha)$ is a continuous function of α . The graph of $f(\alpha)$ versus α , called the multifractal spectrum, typically has a parabolic concave downward shape, with the range of α -values increasing with the increase in the heterogeneity of the measure. The minimum scaling exponent $f(\alpha_{q+})$ corresponds to the most concentrated region of the measure, and the maximum exponent $f(\alpha_{q-})$ corresponds to the rarefied regions of the measure. The connection between the scaling exponents τ_q and $f(\alpha)$ can be made through a Legendre transformation. In this work, however, the functions α_q and $f(\alpha)$ were obtained following

Chhabra and Jensen (1989) with the equations:

$$\alpha(q) \propto \frac{\sum_{i=1}^{N(\delta)} \mu_i(q, \delta) \log[\mu_i(\delta)]}{\log(\delta)} \quad (4a)$$

$$f(\alpha(q)) \propto \frac{\sum_{i=1}^{N(\delta)} \mu_i(q, \delta) \log[\mu_i(q, \delta)]}{\log(\delta)} \quad (4b)$$

The scaling function, τ_q is also related to the generalized fractal dimension (Hentschel and Procaccia, 1983), which can be defined by Equations 5a. In fact, the concept of generalized dimension, D_q , corresponds to the scaling exponent for the q^{th} moment of the measure. Moreover, the generalized dimensions can be also defined by Equation. Note, however, that using Equations (5a or 5b) D_1 becomes indeterminate because the value of the denominator is zero. Therefore, for the particular case that $q = 1$, Equation 5c is used.

$$D_q = \tau(q)/(q-1) \quad (5a)$$

$$D_q = \lim_{\delta \rightarrow 0} \frac{1}{q-1} \frac{\log[\chi(q, \delta)]}{\log \delta} \quad (5b)$$

$$D_1 = \lim_{\delta \rightarrow 0} \frac{\sum_{i=1}^{n(\delta)} \chi_i(1, \delta) \log[\chi_i(1, \delta)]}{\log \delta} \quad (5c)$$

For a monofractal, D_q is a constant function of q , so no additional information is obtained by examining higher moments. However, for multifractal measures, the relationship between D_q and q is not constant. In this case, the most frequently used generalized dimensions are D_0 for $q = 0$, D_1 for $q = 1$ and D_2 for $q = 2$, which are referred to as capacity, information (Shannon entropy) and correlation dimension, respectively.

The capacity or box-counting dimension, D_0 , is the scaling exponent of the number of non-empty segments. Thus, it is independent of the quantity of mass in each box, but takes into account the fact that the segments are occupied or not. The information dimension, D_1 , gives the probability of occupation of the i^{th} segment of size δ , without taking into account the way in which the measure is distributed within each of these segments. Thus, D_1 provides a physical characterization, indicating how heterogeneity changes across a certain range of scales, and it is also related to the Shannon entropy equal. The correlation dimension, D_2 , describes the uniformity of the measure values among intervals.

The generalized dimension, D_q , is widely used for the comprehensive study of multifractals. Differences between D_q allow comparison of the complexity between measured soil ECa data sets. In homogeneous structures D_q are close, whereas in a monofractal they are equal.

ANOVA analysis was performed to compare multifractal parameters from data sets taken in horizontal and vertical

dipole orientations and also the successive transects recorded. Statistical analyses were done using SAS scientific software, version 8.0 (SAS, 1999).

3.- Results and discussion

3.1.- Experimental results

Figure 1 shows the results of five successive records obtained in horizontal dipole position. The range of ECa-H values was relatively low, from about 7 to 12 mS m⁻¹. This is in accordance with the temperate humid climate of the studied regions, which impedes any salt accumulation in the soil profile. Moreover, there were no significant differences in the mean values of either ECa-H or ECa-V between the five different transects recorded.

Although the general spatial trend of the ECa recorded along the five transects is similar, the successive data sets are not superposed. The main differences occur when ECa values peak positively or negatively with respect to the average trend at various positions in the profile. In other words, Typical ECa data sets recorded at the decimeter scale appears noisy.

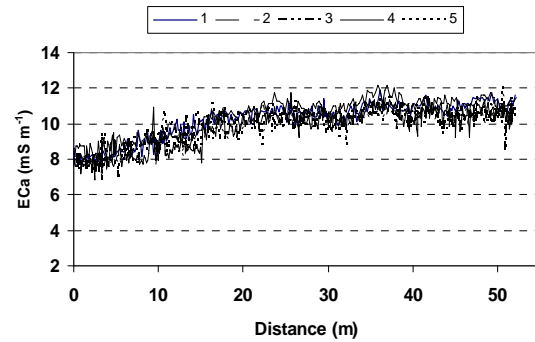


Fig. 1. Spatial variation of ECa-H (i.e. horizontal dipole orientation) for the five replications measured along a transect

The noise observed in particular transects shown in Figure 1 is irrelevant or only weakly relevant to ECa data analysis. It can be attributed to the process of the automatic data collection that results in low-level data errors. On the other hand, differences in ECa values between successive transects mainly arise from small deviations from the pathway followed by the EM38 sensor, which hardly can be impeded or avoided during the experimental work.

3.2.- Multifractal analysis

The distribution of a measure is considered fractal (mono- or multifractal) when the partition function for successive moments can be fitted by power law functions (Evertsz and Mandelbrot, 1992). Therefore, plots of the normalized measure $\chi(q, \delta)$ versus measurement scale, δ , were examined, for all the statistical moments of interest, to find out whether ECa obeyed or not power law scaling. For moment orders in the range between $q = +5$ and $q = -$

5, the logarithm of $\chi(q, \delta)$ versus the logarithm of δ fitted a linear model when the partition function was constructed for successive box sizes in steps of 2^k , $k=0$ to $k=7$. Consequently, partition functions have been estimated in the range of linear behaviour, involving box sizes limited to $0 < k < 7$. An example is shown in Figure 2. Moreover, as shown in this Figure, the parameter q of Equations (4) and (5) was chosen between -5 and $+5$ in increments of 0.5 .

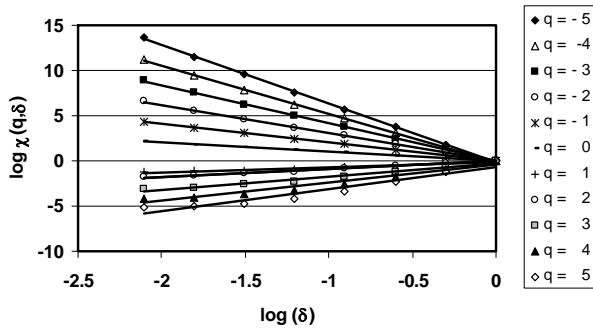


Fig. 2. An example of log–log plots of the partition function, $\chi(q, \delta)$, versus measurement scale, δ

The singularity spectrum was estimated by Equations 4a and 4b, taking a $R^2 = 0.90$ value for the determination coefficient, as a threshold, so that pair of values $f(\alpha)$ versus α below this threshold were not accepted. Following this rule, the range of negative moments used to compute $f(\alpha)$ - α plots was $\Delta q_- = -5.0$ for all the data sets studied, but the range of positive moments Δq_+ varied between 1.5 and 2.5. Singularity spectra were more or less asymmetric, concave down parabolic curves and for all the studied CEa profiles the right branch was longer than the left branch. Examples of singularity spectra are shown in Figure 3.

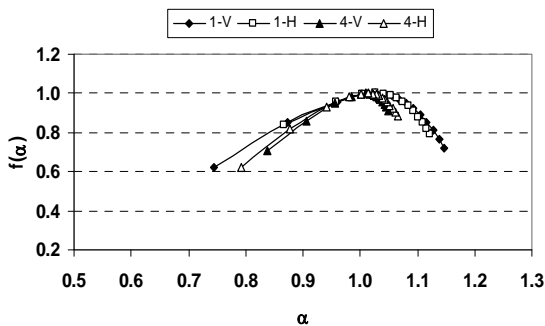


Fig. 3. Selected examples of singularity spectra. (1 and 4 are profile numbers, V and H are vertical and horizontal dipole orientations)

In a homogeneous fractal system the $f(\alpha)$ spectra would be reduced to a single point, therefore, $f(\alpha)$ - α plots in Figure 3 support the hypothesis of singular behavior of the ECa measured along profiles.

Several multifractal parameters obtained from the singularity spectra are listed in Table 1. The Hölder

exponent of order zero, α_0 , varied between 1.011 and 1.027 and determination coefficients in estimating α_0 were 1.000. For α_{-5} and α_{+5} , determination coefficients were 0.998 and 0.967, respectively. Therefore, shape and asymmetry and goodness of fit statistics of the singularity spectra showed the scaling properties of ECa can be fitted reasonably well with multifractal parameters.

In addition, shape and asymmetry of the $f(\alpha)$ - α spectrum can be employed to assess the heterogeneity of a distribution. Also, the width or amplitude of the singularity spectrum, $(\alpha_{q-} - \alpha_{q+})$, i.e. $(\alpha_{-5} - \alpha_5)$, is an indicator of heterogeneity, because it provides information on the diversity of the scaling exponents of a measure. So, the wider the $f(\alpha)$ spectrum is, the higher is the heterogeneity in the scaling indices. Differences in the width of the measure were higher between successive profiles than between measurements taken in vertical and horizontal modes of a given profile.

The presence of extremely high and extremely low data values and dominance of either low or high data are related to the left ($q \gg 1$) and right ($q \ll -1$) parts of the $f(\alpha)$ spectrum, respectively. For ECa profiles, the left branch of the $f(\alpha)$ - α spectrum was wider than the left branch. Asymmetry toward the left indicates dominance of the lowest singularity exponents, α . In general, the left side was also longer than the right side, revealing that the geometrical size of points with the smallest exponents, α , was smaller. The opposite was true for the narrower and shorter right side of the singularity spectrum. This suggest dominance of lowest ECa values along de measured profiles and that these were quite similar to each other, as compared to the highest ECa values that were less frequent and showed more differences between one another along the profile.

Because α_{min} values of all the $f(\alpha)$ - α plots were computed for a similar moment (i.e. $\Delta q_- = -5.0$) and α_{max} values correspond to diverse moments ($1.5 \leq \Delta q_+ \leq 2.5$), singularity spectra obtained from ECa measurements can be best characterized by parameter $(\alpha_{-5} - \alpha_0)$ as well as the by the Hölder exponent, α_0 .

The generalized dimension functions, D_q , were estimated in the range of q moments $-5 \leq q \leq 5$ with Equation (5b), except for $q=1$, where Equation (5c) was used. As expected, coefficients of determination were highest for $q = 0$ ($R^2=1.00$) and decreased with increased $|q|$. Thus for the studied ECa profiles the values of R^2 were higher than 1.000, 0.993, 0.999, and 0.932, for $q = 1, q = 2, q = -5,$ and $q = 5$, respectively. Examples of Rényi dimension spectra; D_q , calculated for 0.5 q steps in the range of moments $q = -5$ to $q = 5$ together with their standard error bars are shown in Figure 4. Rényi spectra follow a typical monotonically decreasing trend with increasing q values, which can be described by a sigma shaped curve. The D_q function crosses through 1.0 at $q=0$ and approaches minimum and maximum values as $q \gg 1$ and $q \ll -1$, respectively. The absolute differences $(D_0 - D_q)$ notably increase as the absolute value of q grows in the two branches of the sigma-shapes curves. Again, these results

clearly support the hypothesis of singular behavior of ECa data series.

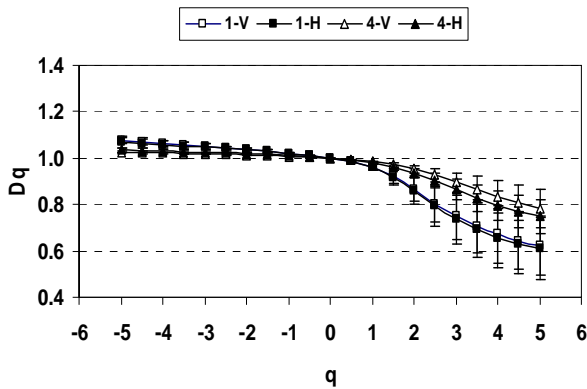


Fig. 4. Selected examples of generalized dimension functions. (1 and 4 are profile numbers, V and H are vertical and horizontal dipole orientations)

The difference $\Delta D_q = (D_{-5} - D_5)$ between the most negative ($q = -5$) and the most positive ($q = 5$) moments has been also employed as a measure of heterogeneity (e.g. Vidal Vázquez et al., 2013). It is apparent that the curvature of the generalized dimension, D_q , was always much higher for positive than for negative values of q . This branch of the Rényi spectra corresponds to the smallest concentrations of the measure. Such result is in accordance with the fact that in general the singularity spectra had a wider left branch (Figure 3).

Table 1. Selected parameters obtained from the generalized dimension and the multifractal spectrum

Prof.	$(D_{-5} - D_5)$	Generalized dimension			
		D_{-5}	D_5	D_1	
1-H	0.457	1.068 ± 0.011	0.611 ± 0.068	0.958 ± 0.007	
1-V	0.451	1.076 ± 0.008	0.625 ± 0.066	0.959 ± 0.006	
2-H	0.427	1.097 ± 0.012	0.670 ± 0.054	0.949 ± 0.007	
2-V	0.449	1.093 ± 0.010	0.644 ± 0.051	0.944 ± 0.007	
3-H	0.165	1.026 ± 0.003	0.861 ± 0.038	0.988 ± 0.002	
3-V	0.203	1.022 ± 0.002	0.819 ± 0.045	0.988 ± 0.002	
4-H	0.286	1.035 ± 0.004	0.749 ± 0.038	0.980 ± 0.001	
4-V	0.242	1.026 ± 0.002	0.785 ± 0.043	0.985 ± 0.002	
5-H	0.285	1.048 ± 0.005	0.763 ± 0.051	0.976 ± 0.004	
5-V	0.336	1.046 ± 0.005	0.709 ± 0.050	0.969 ± 0.004	
Prof.	q_+	q_-	Singularity spectrum		
			α_0	α_5	$(\alpha_5 - \alpha_0)$
1-H	1.5	-5	1.027 ± 0.006	1.123 ± 0.045	0.096
1-V	2	-5	1.027 ± 0.005	1.147 ± 0.030	0.120
2-H	2	-5	1.038 ± 0.008	1.165 ± 0.042	0.127
2-V	2	-5	1.040 ± 0.007	1.153 ± 0.032	0.113
3-H	3	-5	1.009 ± 0.003	1.049 ± 0.009	0.040
3-V	2.5	-5	1.009 ± 0.002	1.039 ± 0.011	0.030
4-H	2.5	-5	1.014 ± 0.001	1.066 ± 0.018	0.052
4-V	2.5	-5	1.011 ± 0.002	1.049 ± 0.013	0.039
5-H	2	-5	1.018 ± 0.004	1.086 ± 0.020	0.068
5-V	2	-5	1.021 ± 0.003	1.079 ± 0.017	0.058

(Prof.= profile; H= horizontal; V = vertical; D_{-5} , D_1 , and D_5 = generalized dimensions for moments $q = -5$, 1 and 5, respectively; $(D_{-5} - D_5)$ = maximum width of D_q function; α_0 and α_5 = Hölder exponent of order zero, and singularity strength for $q = -5$; $(\alpha_5 - \alpha_0)$ = width of the right branch of the $f(\alpha)$ spectrum)

The capacity dimension, D_0 , was not significantly different from 1, in all of the 10 ECa data series studied. The entropy or information dimension, D_1 , varied between 0.944 and 0.988 (Table 1). D_0 and D_1 would take the same value for a monofractal scaling type. Again the multifractal behavior of the replicated ECa data sets is very clearly expressed in the shape and parameters derived from the generalized dimension, supporting the hypothesis of its singular behavior.

Both, the singularity spectrum and the generalized dimension spectrum confirmed that multifractal models, fit reasonably well with ECa transects. The multifractal approach gives a good description of the spatial variability of the replicated transects of electrical conductivity, measured in vertical (ECa-V) and horizontal (ECa-H) dipole orientations. The transect studied can be considered representative of the main pedological and topographical conditions at the CIAM experimental farm. Therefore, the scaling properties of the successive ECa measurements along this transect embody realistic situations consistent with observations at the level of a small field.

The spatial variability in ECa, reflects, on the one hand the effect of the main soil factors from which it depends and on the other hand the effect of noise arisen from the electronic data acquisition system. First, the movement of electrons through bulk soil is complex. Electrons may travel through soil water in macropores, along the surfaces of soil minerals (i.e. exchangeable ions), and through alternating layers of particles and solution (e.g. Corwin and Lesch, 2005; Allred et al., 2008). Therefore, multiple factors contribute to soil variability at several scales. Subsequently, the scaling heterogeneity or multifractality observed in ECa transects may result from the amount and connectivity of soil water (e.g. bulk density, structure, water potential, precipitation, timing of measurement), soil aggregation (e.g. cementing agents such as clay and organic matter, soil structure), electrolytes in soil water (which in our study conditions mainly means exchangeable ions, soil water content, because salinity is negligible), and the conductivity of the mineral phase (e.g. types and quantity of minerals, degree of isomorphic substitution, exchangeable ions). Second, the multifractality of the studied ECa transects might also partly be the result of noise originated during the automatic data collection process with the EM38 device. Thus, acute ECa peaks observed in Figure at the decimeter scale, obviously contributing to scaling heterogeneity, are probably associated to low-level data errors. All these factors operate and interact at closely related scales giving rise to the observed ECa spatial variability.

Several multifractal parameters gathered from the singularity spectrum and the generalized dimension spectrum of the ECa transects measured in vertical (ECa-V) and horizontal (ECa-H) dipole orientation were compared by ANOVA analysis. Noteworthy, no significant differences ($P < 0.05$) were found between multifractal parameters of ECa-H and ECa-V transects for any of the studied repetitions. Also no significant differences were found between the respective mean ECa-

H and ECa-H measured in this study.

ANOVA analysis was also performed to evaluate differences in mean values of multifractal parameters between the five replicated transects studied; in this case ECa-V and ECa-H data sets were considered as repetitions as they were not statistically different. Mean values showed no significant differences between the five transects. In opposite, several multifractal parameters were significantly different ($P < 0.05$) when the five repetitions were compared as summarized in Table 2.

The most sensitive parameters to differentiate between replicated transects were the Hölder exponent of order zero, α_0 , ($F = 131.29$, $P < 0.000$), the generalized dimension for $q = -5$, the most negative q moment computed, D_{-5} , ($F = 95.84$, $P < 0.000$), the entropy dimension, D_1 , ($F = 58.51$, $P < 0.000$) and the singularity strength for $q = -5$ ($F = 42.56$, $P < 0.000$). In other words, multifractal parameters derived either from the central part or the branches with negative q moments have been shown as most sensitive to differentiate between replicated ECa-profiles automatically recorded over our transect of about 52 m.

Table 2. Comparison of differences in multifractal parameters between successive ECa transects by ANOVA analysis

	$(D_{-5} - D_5)$	D_{-5}	D_5	D_1	α_0	α_{-5}	$(\alpha_{-5} - \alpha_0)$
F	40.83	96.84	22.76	58.51	131.29	42.56	25.09
P	0.001	0.000	0.002	0.000	0.000	0.000	0.002

(F = F value; P = significance; symbols for multifractal parameters as in Table 1)

Further research should be conducted to validate the usefulness of multifractal analysis for providing information on ECa inner structure measured along one dimensional transects or two dimensional fields. This information could be helpful to better assess the use of soil ECa as secondary information, thus as a surrogate method for detection of spatial variation of soil properties.

4.- Conclusions

Apparent electrical conductivity continuously recorded along small transects using a mobile GPS-based system exhibited multifractal behaviour both in the vertical and horizontal dipole orientations. All the singularity spectra studied were characterized by a wider left branch, whereas the generalized dimension spectra had a wider right branch, which correspond to the smallest concentrations of the measure.

Multifractal parameters gathered from the singularity spectrum and the generalized dimension spectrum showed not significant differences between ECa data sets acquired in the vertical or the horizontal orientations for any of the studied transects. However, multifractal parameters were significantly different when data sets obtained during successive ECa records were compared.

Acknowledgments. This work was funded in part by Spanish Ministry of Science and Innovation (MICINN) in the frame of project CGL2009-

13700-C02.

5.- References

- Allred, B.J., J.J. Daniels, y M.R. Ehsani, 2008. *Handbook of agricultural geophysics*. : CRC Press. Boca Raton, FL, USA.
- Chhabra, A.B., and R. V. Jensen, 1989. Direct determination of the $f(\alpha)$ singularity spectrum. *Phys. Rev. Lett.* 62, 1327-1330.
- Corwin, D.L. and S.M. Lesch, 2005. Characterizing soil spatial variability with apparent soil electrical conductivity: I. Survey protocols. *Comp. Electron. Agric.* 46 (1-3), 103-133.
- Corwin, D.L., S.M. Lesch, J.D. Oster and S.R. Kaffka, 2006. Monitoring management-induced spatio-temporal changes in soil quality through soil sampling directed by apparent electrical conductivity. *Geoderma* 131, 369-387.
- Everstz, C.J.G., and B. B. Mandelbrot, 1992. Multifractal measures. In *Chaos and Fractals*. Peitgen, H., H. Jürgens, and D. Saupe (ed.), Springer, Berlin, 921-953.
- Geonics Limited, 1999. *EM38 ground conductivity meter-operating manual*. Mississauga, Ontario, Canadá.
- Halsey, T.C., M.H. Jensen, L. P. Kadanoff, I. Procaccia, and B. I. Shraiman, 1986. Fractal measures and their singularities: The characterization of strange sets. *Physical Review*, A, 33, 1141-1151.
- Hentschel, H.G.E., and I. Procaccia. 1983. The infinite number of generalized dimensions of fractals and strange attractors. *Physica D.*, 8, 435-444.
- Lesch, S.M., D.J. Strauss, and J.D. Rhoades, 1995. Spatial prediction of soil salinity using electromagnetic induction techniques: I. Statistical prediction models: a comparison of multiple linear regression and cokriging. *Water Resour. Res.* 31, 373-386.
- Martínez, G., K. Vanderlinden, J.V. Giráldez, A.J. Espejo, E. Rodríguez, R. Ordóñez, and J.L. Muriel, 2009. Use of apparent electrical conductivity as secondary information for soil organic carbon spatial characterization, in: *Estudios en la Zona no Saturada del Suelo, Vol IX*, O. Silva et al. (eds.), Barcelona.
- SAS-Statistical Analysis System, SAS Institute, 1999. Users SAS Institute. NC. USA.
- Shmulik, P.F., 2005. Soil properties influencing apparent electrical conductivity: A review. *Comput. Electron. Agr.* 46, 45-70.
- Soil Survey Staff. 2010. *Keys to Soil Taxonomy. 11th Edition*. Natural Resources Conservation Service. Washington. DC. 338.
- Tarquis, A.M., N.R.A. Bird, A.P. Whitmore, M.C. Cartagena, and Y. Pachepsky. 2008. Multiscale Entropy-based Analysis of Soil Transect Data. *Vadose Zone J.* 7, 563-569.
- Vidal Vázquez, E, O.A. Camargo, S.R. Vieira, J.G.V. Miranda, J.R.F. Menk, G.M. Siqueira, J.M. Mirás Avalos, and A. Paz González, 2013. Multifractal analysis of soil properties along two perpendicular transects. *Vadose Zone J.* 12, 1-13.